JACS
JOURNAL OF THE AMERICAN CHEMICAL SOCIETY
Communication
Cite This: J. Am. Chem. Soc. XXXX, XXX, XXX−XXX
pubs.acs.org/JACS

New Design Paradigm for Color Control in Anodically Coloring Electrochromic Molecules

Dylan T. Christiansen,[†] Aimée L. Tomlinson,[‡] and John R. Reynolds*[,†]

[†]School of Chemistry and Biochemistry, School of Materials Science and Engineering, Center for Organic Photonics and Electronics, Georgia Tech Polymer Network, Georgia Institute of Technology, Atlanta, Georgia 30332, United States

[‡]Department of Chemistry/Biochemistry, University of North Georgia, Dahlonega, Georgia 30597, United States

Supporting Information

ABSTRACT: A new paradigm is established for the design of conjugated anodically coloring electrochromic molecules. It is shown that through crossconjugation the electronic energy levels of the radical cation state may be controllably tuned independent of the neutral state. It is shown how cross-conjugation can be used to tune the radical cation state independent of the neutral state. Manipulating the oscillator strengths of radical cation transitions allows for tuning of the color by shifting the λ_{max} of the low-energy absorption by over 400 nm. The neutral states of these molecules are UV absorbing, providing solutions that are colorless with L*a*b* values of 100, 0, 0. They are oxidized to vibrantly colored radical cations with absorptions that span the visible spectrum, creating green, yellow, and red chromophores. These molecules are then mixed to create transmissive, colorless blends that switch to opaque black solutions.

Electrochromism is the change of color upon the application of an electrochemical potential leading to prospective uses in full color passive displays, energy saving tinted windows, and dimmable glasses, goggles, and visors for military and/or recreational use.[1−5] Easily oxidized, cathodically coloring, organic polymer electrochromes have been the focus of a large thrust of research due to their solution processability, mechanical flexibility, device bistability, and access to a variety of primary and secondary colors. Cathodically coloring electrochromic polymers are colored in the neutral state and oxidize to be transmissive. Fine control of the visible spectra, and ultimately color, of these materials has been accomplished through the variation of heterocycle choice, electron-rich/poor character, steric strain, and copolymerization.[6−10] While cathodically coloring electrochromic polymers have several advantages, the oxidized, transmissive states of these materials have residual red-light absorption, leaving a light blue tint in the film.[11,12] To overcome this challenge, this work reports on electron-rich molecules that are UV absorbing in the neutral state and form vibrantly colored radical cations states upon oxidation.

In contrast to cathodically coloring polymers, anodically coloring electrochromics are colorless in the neutral state and oxidize to colored species. In the field of anodically coloring organic electrochromics there is a knowledge gap on how absorption in the charged state is controlled.[13−18] This work demonstrates how to bridge this gap with a fundamental approach to manipulating the electronic energy levels of odd-electron organic systems.[19,20] In this work, it is shown that electron-rich/deficient moieties cross-conjugated into the chromophore can be utilized for manipulating radical cation energy levels and ultimately controlling absorption and color.

Figure 1 details the structures designed to create a set of anodically coloring electrochromes where the neutral and radical cation states' optical gaps are controlled independently. Here, novel UV-absorbing discrete chromophores based on a 2-thiomethyl-ethylenedioxythiophene coupled to a 4-methoxybenzene derivative are introduced, giving anodically coloring electrochromes (ACEs). Color control is achieved by altering the substitution on the benzene moiety, leading to radical cations that absorb across the visible spectrum. While the absorption of the neutral state can be tuned through manipulating the electron-donating/withdrawing character of the substituent in the *para*-position (red), it is largely unaffected by the substituents in the *meta*-position (green). The chromophores examined in this study increase in electron density donated in the *meta*-position of the benzene from **ACE1** to **ACE4**. The *para*-position moiety remains constant to add electron density, cap reactive ends, and maintain a neutral state with a similar optical gap. This study examines the effectiveness of altering the radical cation absorption independent of the neutral absorption through tailoring the electron richness in the *meta*-positions.

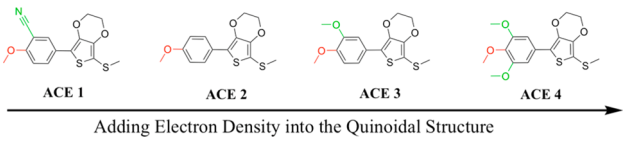

Figure 1. Key molecules are listed in order of increasing electron-donating character of the moieties in the *meta*-position.

In order to guide experiment and probe the design paradigm from a molecular orbital perspective, time-dependent density functional theory (TDDFT) calculations were performed on these molecules and theoretical spectra were generated for the neutral and radical cation states of the molecules (see Figure 2). As can be seen in comparing the solid curves, there is

Received: February 19, 2019

DOI: 10.1021/jacs.9b01507
J. Am. Chem. Soc. XXXX, XXX, XXX−XXX

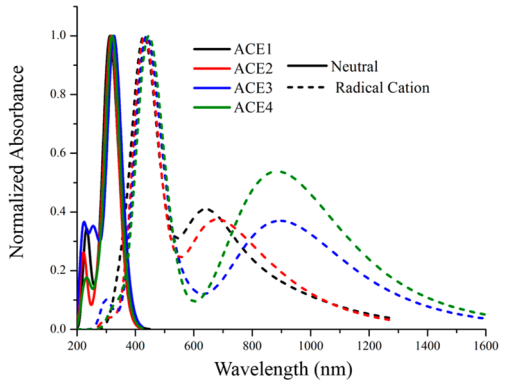

Figure 2. TDDFT-calculated spectra for the neutral and radical cation states for the molecules in this study.

minimal change in the absorbance of the neutral molecules upon the addition of electron-rich moieties at the *meta*-position. All of the spectra have a λ_{max} in the UV with absorption onsets of ~400 nm. However, when examining the radical cation spectra, there are stark differences. While the high-energy absorption appears to be consistent between these molecules, there is a significant alteration in energies between the long-wavelength transitions as evidenced by a red-shifting of this peak. There is a particularly large red-shift going from **ACE2** to **ACE3**, upon addition of a methoxy group to the *meta*-position, which is consistent with the energy levels, oscillator strengths, and frontier molecular orbitals (FMOs), Figure S1, Table S1, and Figure S2.

A detailed analysis of the TDDFT oscillator strengths provides some insight into the absorption differences for these radical cations, as seen in Figure S1 and Table 1 (an extensive list of transitions can be seen in Table S1). In all cases, the transition that carries the largest oscillator strength (f) is the SOMOα → LUMOα (Sα → Lα), which remains relatively unchanged (434–435 nm) until **ACE4** (449 nm). It is the remaining significant transitions (those possessing $f \geq 0.1$) that are believed to control the color. For **ACE1**, there was a transition found for the SOMO-1β → LUMOβ (S-1β → Lβ) corresponding to 636 nm. In the case of **ACE2**, the Sβ-1 → Lβ transition was slightly red-shifted at 650 nm peak and the appearance of a SOMOβ → LUMOβ (Sβ → Lβ) at 846 nm with a lower oscillator strength. The oscillator strength for the Sβ → Lβ transition for **ACE3** increased relative to the S-1β → Lβ transition and red-shifts to 863 nm. Finally, **ACE4** indicated the largest red-shift for the Sβ → Lβ transition at 900 nm and a further decrease in the oscillator strength associated with the S-1β → Lβ transition. Interestingly, **ACE4** had a second high-energy transition of significant oscillator strength in the visible at 406 nm associated with the S-3β → Lβ transition.

Table 1. Oscillator Strengths and Transitions of Radical Cations

molecule	λ (nm)	f	dominant transition
ACE1	636	0.24	S-1β → Lβ
ACE1	435	0.52	Sα → Lα
ACE2	847	0.10	Sβ → Lβ
ACE2	650	0.22	S-1β → Lβ
ACE2	434	0.63	Sα → Lα
ACE3	863	0.13	Sβ → Lβ
ACE3	690	0.15	S-1β → Lβ
ACE3	434	0.63	Sα → Lα
ACE4	900	0.28	Sβ → Lβ
ACE4	449	0.50	Sα → Lα
ACE4	406	0.14	Sβ-3 → Lβ

Figure 3 describes electronic structures and representative spectra for a pair of ideal anodically coloring molecules in the radical cation state. In both cases the highest oscillator strength transitions correspond most strongly with the Sα → Lα excitation (a and c). As there is a minimal energy difference in this transition between the molecules, minimal red-shifting of this absorption peak is observed. For an electron-poor system, the low-energy absorption is dominated by the Sβ-1 → Lβ excitation (b). As electron density is added to the chromophore, the Sβ → Lβ excitation takes over as the dominate contributor to the transition, leading to a red-shift in absorption (d).

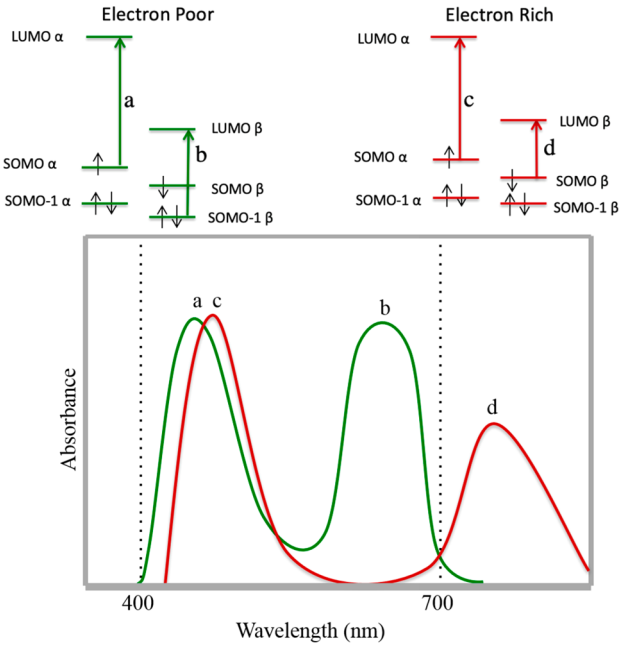

Figure 3. Concept diagram showing electronic structures and representative spectra of allowed transitions in ideal conjugated molecular electrochromes in the radical cation state.

When probing these molecules experimentally, the observations are consistent with the trends seen in the calculations. Figure 4 details the differential spectroelectrochemistry results performed in electrolyte solution using an optically transparent thin layer electrode (OTTLE), where a platinum screen is used as a working electrode to allow light to pass through the cell. In this experiment the neutral spectrum is subtracted as a baseline in order to remove the noise caused by the screen. A schematic of the OTTLE is available in Figure S3. Comparisons of the calculated and experimental spectra are available in Figure S4. It is evident that the calculations accurately depicted the location of the peaks and the red-shifting trend seen in the low-energy absorption upon the incorporation of electron-rich substituents. This ability to rationally shift the low-energy absorbance allows access to a large variety of colors through minimal changes in chemical structure. The bright green of the cyano-containing **ACE1** is due to the combination of two peaks in the visible with λ_{max} at 461 and 653 nm and a

DOI: 10.1021/jacs.9b01507
J. Am. Chem. Soc. XXXX, XXX, XXX–XXX

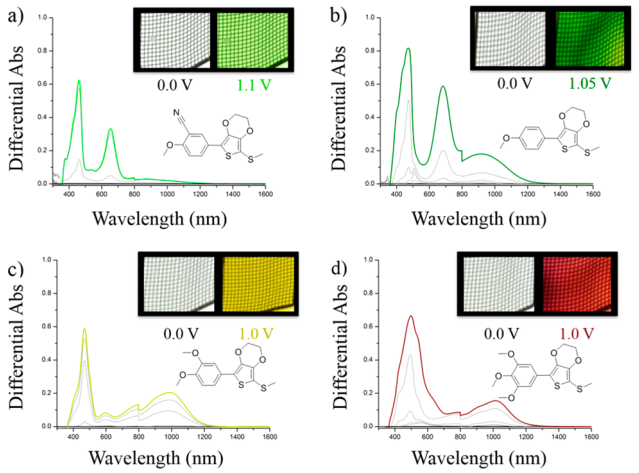

Figure 4. Differential spectroelectrochemistry performed with an OTTLE with photographs in the insets at the extreme potentials as noted. (a) **ACE1**, (b) **ACE2**, (c) **ACE3**, (d) **ACE4**.

transmission window between 500 and 570 nm. Upon removing the electron-withdrawing group, there is a small shift in absorbance of the radical cation peaks for **ACE2** with λ_{max} at 471 and 683 nm and a more red-shifted window of transmission at 520−690 nm, yielding a more saturated green color. The formation of the shoulder in the NIR for **ACE2** at 915 nm is the first evidence of contribution from the Sβ → Lβ transition. As more electron density is added to the chromophore for **ACE3**, the contribution from the Sβ-1 → Lβ becomes suppressed with only a small absorbance observed at 597 nm. Large absorbances at 469 and 986 nm give a bright yellow color, with only one strong transition located in the visible. When examining the most electron-rich system, **ACE4**, the low-energy peak red-shifts to 1013 nm as predicted, and there is an observed red-shift and broadening of the high-energy peak at 496 nm. The increased breadth of the high-energy radical cation peak when comparing **ACE3** with **ACE4** causes a color change from a vibrant yellow to a deep red. This broadening can be attributed to the combination of the S-1β → Lβ and S-3β → Lβ transitions. The calculated and experimental data comparisons are collated in Table S2.

Cyclic voltammetry (CV) and differential pulse voltammetry (DPV) were used to probe cation-radical formation, and the results are shown in Figure S5. All molecules exhibit quasi-reversible radical cation oxidations, but Figure S5C indicates that **ACE4** has two peaks indicative of the formation of a dication. This oxidation renders the electrochemistry irreversible and causes the formation of a new electroactive species, although it can be reduced back to neutral/colorless on the OTTLE when applying a reducing potential for an extended period. Formation of the dication would also corroborate with the apparent red-shift and broadening observed for the high-energy radical cation peak, as it is a combination of absorption from radical cations and dications.

The color neutrality and transmissivity of the neutral state and the color vibrancy obtained through chemical oxidative doping are shown in Figure 5. This experiment was performed in 250 μM solutions with $Fe(OTf)_3$ as the oxidizing dopant. Photographs are taken in borosilicate vials before exposure to air. Color for these materials was quantified using the CIELAB color space.[21] The a*b* plot shows the quantitative change in color upon sequential oxidative doping as calculated from the

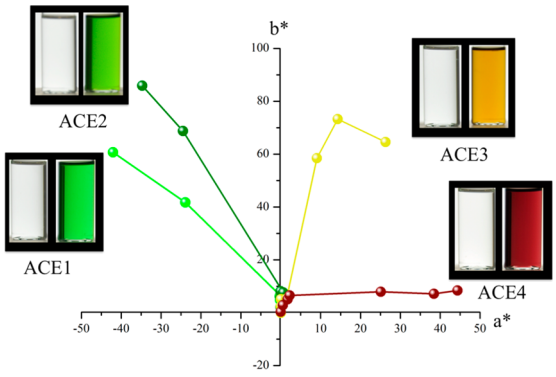

Figure 5. Evolution of colorimetry of oxidatively doped solutions of the ACE molecules. The solutions are 250 μM of each compound and $Fe(OTf)_3$ is the dopant.

UV−vis absorbance spectra of neutral and doped solutions. All calculated L*a*b* values for the neutral compounds are (100, 0, 0), which can be observed in the photographs as being completely color neutral and transmissive. Each of these compounds is oxidized to a vivid color that, in combination, covers a wide area in the color space. From the spectra in Figure S6, it can be noted that the absorptions generated with chemical oxidation are similar to what is seen on the OTTLE, with the exception of **ACE4**. This molecule has a single peak upon oxidation with a λ_{max} at 496 nm. This observation is indicative of the molecule oxidizing directly to the dication upon chemical doping, as there is no spectral evidence of radical cation formation. This result is not unexpected given the proximity of the oxidation peaks as measured by DPV.

A 1:1 mixture of **ACE2** and **ACE4** was created, and the differential spectroelectrochemistry and photography are detailed in Figure 6. As can be seen from the photography,

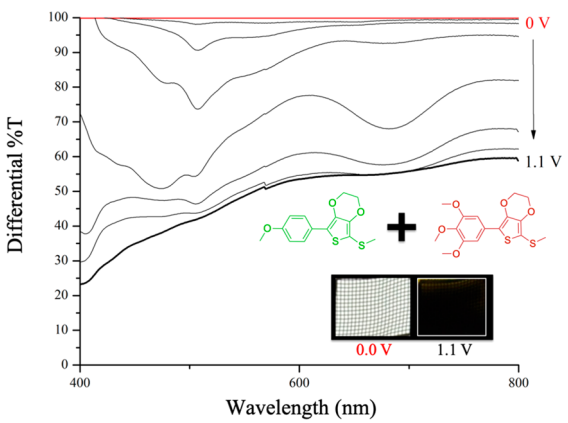

Figure 6. Differential spectroelectrochemistry performed with an OTTLE of a 1:1 mixture of **ACE2** and **ACE4** with photographs in the inset at the extreme potentials as noted.

the mixture changes from a color-neutral, transmissive solution to an opaque black. One can imagine that the blends can be adjusted to create browns and other secondary colors from only a few molecules, as the library of ACE molecules is expanded.

In conclusion, a new design paradigm is introduced for creating anodically coloring molecules where there is synthetic control on the absorption of the oxidized state. Radical cation absorption is tailored independent of the neutral absorption

DOI: 10.1021/jacs.9b01507
J. Am. Chem. Soc. XXXX, XXX, XXX−XXX

using electron-donating/withdrawing moieties cross-conjugated into the chromophore structure. Quantum chemical calculations give insight into how energy levels are manipulated to control transition dominance in odd-electron systems and guide molecular design to create new anodically coloring electrochromic molecules. It has been shown that these molecules have overcome the contrast barrier present in the field of organic electrochromism while maintaining a wide variety of tunable colors and secondary blends. As the collection of available ACE compounds expands, these materials have prospects toward moving to solid-state devices by incorporation into polymers or adding cross-linkable moieties to create an insoluble network. Additionally, these molecular design principles can be used in other conjugated organic systems for tuning radical cation electronic structures.

■ ASSOCIATED CONTENT

Supporting Information

The Supporting Information is available free of charge on the ACS Publications website at DOI: 10.1021/jacs.9b01507.

Supplementary figures, experimental details, synthesis, and primary characterizations (PDF)

■ AUTHOR INFORMATION

Corresponding Author

*reynolds@chemistry.gatech.edu

ORCID

Dylan T. Christiansen: 0000-0002-8673-5870

John R. Reynolds: 0000-0002-7417-4869

Notes

The authors declare the following competing financial interest(s): Electrochromic polymer technology developed at the Georgia Institute of Technology has been licensed to NXN Licensing. J.R.R. serves as a consultant to NXN Licensing.

■ ACKNOWLEDGMENTS

Funding from the Air Force Office of Scientific Research (FA9550-18-1-0184 and FA9550-18-1-0034).

■ REFERENCES

(1) Granqvist, C. G. Electrochromic Materials: Out of a Niche. *Nat. Mater.* **2006**, *5* (2), 89.

(2) Krebs, F. C. Electrochromic Displays: The New Black. *Nat. Mater.* **2008**, *7* (10), 766.

(3) Grätzel, M. Materials Science: Ultrafast Colour Displays. *Nature* **2001**, *409* (6820), 575.

(4) Yang, P.; Sun, P.; Mai, W. Electrochromic Energy Storage Devices. *Mater. Today* **2016**, *19* (7), 394−402.

(5) Qu, H.-Y.; Primetzhofer, D.; Arvizu, M. A.; Qiu, Z.; Cindemir, U.; Granqvist, C. G.; Niklasson, G. A. Electrochemical Rejuvenation of Anodically Coloring Electrochromic Nickel Oxide Thin Films. *ACS Appl. Mater. Interfaces* **2017**, *9* (49), 42420−42424.

(6) Dyer, A. L.; Thompson, E. J.; Reynolds, J. R. Completing the Color Palette with Spray-Processable Polymer Electrochromics. *ACS Appl. Mater. Interfaces* **2011**, *3* (6), 1787−1795.

(7) İçli, M.; Pamuk, M.; Algi, F.; Önal, A. M.; Cihaner, A. Donor−Acceptor Polymer Electrochromes with Tunable Colors and Performance. *Chem. Mater.* **2010**, *22* (13), 4034−4044.

(8) Shin, H.; Kim, Y.; Bhuvana, T.; Lee, J.; Yang, X.; Park, C.; Kim, E. Color Combination of Conductive Polymers for Black Electrochromism. *ACS Appl. Mater. Interfaces* **2012**, *4* (1), 185−191.

(9) Hassab, S.; Shen, D. E.; Österholm, A. M.; Da Rocha, M.; Song, G.; Alesanco, Y.; Viñuales, A.; Rougier, A.; Reynolds, J. R.; Padilla, J. A New Standard Method to Calculate Electrochromic Switching Time. *Sol. Energy Mater. Sol. Cells* **2018**, *185*, 54−60.

(10) Kerszulis, J. A.; Bulloch, R. H.; Teran, N. B.; Wolfe, R. M. W.; Reynolds, J. R. Relax: A Sterically Relaxed Donor−Acceptor Approach for Color Tuning in Broadly Absorbing, High Contrast Electrochromic Polymers. *Macromolecules* **2016**, *49* (17), 6350−6359.

(11) Christiansen, D. T.; Wheeler, D. L.; Tomlinson, A. L.; Reynolds, J. R. Electrochromism of Alkylene-Linked Discrete Chromophore Polymers with Broad Radical Cation Light Absorption. *Polym. Chem.* **2018**, *9*, 3055−3066.

(12) Bubnova, O.; Crispin, X. Towards Polymer-Based Organic Thermoelectric Generators. *Energy Environ. Sci.* **2012**, *5* (11), 9345−9362.

(13) Yen, H.-J.; Liou, G.-S. Solution-Processable Triarylamine-Based Electroactive High Performance Polymers for Anodically Electrochromic Applications. *Polym. Chem.* **2012**, *3* (2), 255−264.

(14) Liou, G.-S.; Lin, H.-Y. Synthesis and Electrochemical Properties of Novel Aromatic Poly (Amine− Amide) s with Anodically Highly Stable Yellow and Blue Electrochromic Behaviors. *Macromolecules* **2009**, *42* (1), 125−134.

(15) Sezgin, M.; Ozay, O.; Koyuncu, S.; Ozay, H.; Baycan Koyuncu, F. A Neutral State Colorless Phosphazene/Carbazole Hybride Dendron and Its Electrochromic Device Application. *Chem. Eng. J.* **2015**, *274*, 282−289.

(16) Yen, H.-J.; Lin, K.-Y.; Liou, G.-S. Transmissive to Black Electrochromic Aramids with High Near-Infrared and Multicolor Electrochromism Based on Electroactive Tetraphenylbenzidine Units. *J. Mater. Chem.* **2011**, *21* (17), 6230−6237.

(17) Walczak, R. M.; Reynolds, J. R. Poly(3,4-Alkylenedioxypyrroles): The PXDOPs as Versatile yet Underutilized Electroactive and Conducting Polymers. *Adv. Mater.* **2006**, *18* (9), 1121−1131.

(18) Chang, T.-H.; Lu, H.-C.; Lee, M.-H.; Kao, S.-Y.; Ho, K.-C. Multi-Color Electrochromic Devices Based on Phenyl and Heptyl Viologens Immobilized with Uv-Cured Polymer Electrolyte. *Sol. Energy Mater. Sol. Cells* **2018**, *177*, 75−81.

(19) Winkler, S.; Amsalem, P.; Frisch, J.; Oehzelt, M.; Heimel, G.; Koch, N. Probing the Energy Levels in Hole-Doped Molecular Semiconductors. *Mater. Horiz.* **2015**, *2* (4), 427−433.

(20) Png, R. Q.; Ang, M. C. Y.; Teo, M. H.; Choo, K. K.; Tang, C. G.; Belaineh, D.; Chua, L. L.; Ho, P. K. H. Madelung and Hubbard Interactions in Polaron Band Model of Doped Organic Semiconductors. *Nat. Commun.* **2016**, *7* (May), 1−9.

(21) Tkalcic, M.; Tasic, J. F. *Colour Spaces: Perceptual, Historical and Applicational Background*; IEEE, 2003; Vol. *1*.

DOI: 10.1021/jacs.9b01507
J. Am. Chem. Soc. XXXX, XXX, XXX−XXX